Crack Growth Prediction in Girth Welds of Steel Catenary Risers

Ilson P. Pasqualino and Ingrid A. Valeriano
Ocean Engineering Department, COPPE, UFRJ
Rio de Janeiro, RJ, Brazil

Teresinha M.J. Alves
PETROBRAS/CENPES
Rio de Janeiro, RJ, Brazil

ABSTRACT

This study involves the numerical simulation of crack growth in girth welds of steel catenary risers under constant tension and cyclic bending. The modeling was carried out with the aid of a finite elements framework and a fracture mechanics program, which generates the initial crack and updates the model mesh according to the local energy release rate of the crack front nodes. The non-linear analysis comprises three-dimensional model mesh with solid elements, finite rotations, elastic-plastic behavior of the material and the linear theory of fracture mechanics. The numerical results were qualitatively compared with proposed fatigue curve of the British Standard International code.

KEY WORDS: Crack propagation; steel catenary riser; reeling process.

NOMENCLATURE

a	crack growth
C, m	material constants
D	pipe external diameter
D_{sm}	diameter of the pipe middle surface
E	elasticity modulus
G	modulus of the energy release rate vector
$\mathbf{G}$	energy release rate vector
K	stress intensity factor
K_c	critical stress intensity factor
M	longitudinal bending moment
n	hardening parameter
N	number of cycles
t	pipe wall thickness
S_r	stress range
T	axial tension
T_0	yielding tension
x_1, x_2, x_3	global Cartesian coordinates
ε_{eqv}^{p}	equivalent plastic strain
ν	Poisson ratio
σ	normal stress
σ_0	yield stress

INTRODUCTION

One of the most efficient methods of pipeline installation is the reeling laying process that involve pipe onshore welding and pipeline bending over a rigid circular surface (reel) on the vessel. Subsequently, the pipeline is straightened and launched under tension into the sea. The straightening operation may not be required depending on the residual strain in the pipe after the bending phase. They have been successfully used by PETROBRAS in Brazil for installing pipelines up to 1,360 m (4,460 ft) water depth.

However, when the steel catenary riser (SCR) concept is considered in conjunction with these methods, there is some scepticism regarding the impact in the fatigue performance of the pipe caused by possible changes in the material and geometrical properties occurred during installation. Consequently, large scope pipeline installation campaigns may require a second contract for SCR's installation using the J-lay method. The project is then penalized due to the attention required to manage the additional interfaces and the consequent impact in the overall pipeline project schedule and costs.

Bending, unbending, and straightening processes as applied in the current vessels induce to the pipe bending-curvature histories into the plastic range of the material. Although the pipe is usually straightened prior to launch, residual out-of-roundness, residual stresses, changes in material properties due to plasticity, and growing of eventual welding flaws may occur. These effects may have an influence in both ultimate strength and subsequent fatigue performance of the pipeline. Thus, in addition to ultimate strength design, the use of steel catenary risers (SCR's) implies in a careful examination of the possibility of riser failure due to fatigue. In this context, the influence of installation methods involving pipeline material and geometric changes must be taken into account in the evaluation of the riser structural integrity during its operational life.

Fatigue life predictions based on S-N curves could be employed in the preliminary stages of the design. Nevertheless, the necessary confidence to establish a consistent planning for SCR's installations in deepwater should be built upon an experimental program comprising fatigue tests using full-scale pipes and realistic welding processes. In order to assess the possible detrimental effect of such installation procedures into the riser fatigue performance, welded segments of pipe must be bent over a rigid surface, unbent and straightened prior to the cyclic loading test. This experimental program "Plastically Strained SCR's Qualification Program for Installation Methods" is part of a Joint Industry Research Project that has been conducted by COPPE-Federal University of Rio de Janeiro (COPPE/UFRJ) and PETROBRAS with the participation of four other companies (Netto et al., 2000).

A complementary numerical and experimental program "Feasibility of the Reeling Laying Process for SCR's" has also been conducted by COPPE and PETROBRAS. One of the aims of this project is to develop a numerical tool to simulate the propagation of flaws in reeled SCR's. The experimental results will be used to calibrate the theoretical model, so that crack propagation curves may be obtained through a parametric study involving different flaw geometries, materials, loading conditions and pipe dimensions. These curves may be used to develop fatigue design recommendations for reeled SCR's. This work will present the development of the numerical model to simulate a crack growth in girth welds of reeled SCR's under cyclic loading.

NUMERICAL MODEL DESCRIPTION

The fracture mechanics analysis of crack propagation was accomplished with the aid of the finite element method. The framework ABAQUS release 6.1 was employed in the finite element analyses while the fracture mechanics program ZENCRACK was used to generate the initial crack and update the model mesh during propagation.

Numerical Model Geometry

The structure studied is an eight-inch nominal diameter rigid riser with a girth weld fillet at the middle section. The external diameter *D* and wall thickness *t* are equal to 220 mm and 15.35 mm, respectively. It is based on the geometry of the full-scale models constructed for the experimental program "Feasibility of the Reeling Laying Process for SCR's" (Pasqualino, 2001). The butt weld geometry considered in the analysis is showed in the schematic drawing of Fig. 1. The weld chamfer is equal to 60° and the root gap and root face are equal to 3.5 mm and 2 mm, respectively. The heat-affected zone is assumed to extend over 2 mm of the adjacent parent material. According to the full-scale models, the outer surface of the weld was made flush with pipe external surface.

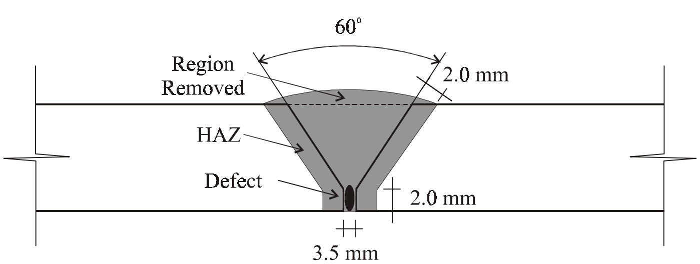

Fig. 1. Girth weld geometry.

The full-scale models were constructed with small defects that are admissible within a weld qualification criterion. The aim of the experimental program is to investigate the adequacy of these criteria to girth welds of reeled SCR's. The full-scale model D08T1A (Pasqualino, 2001) was selected to provide the geometry for the numerical analyses. Its defect is a lack of penetration at the root, as indicated in Fig. 1, with 23 mm length in the hoop direction and 4 mm depth.

Finite Element Mesh

The finite element mesh was generated using three-dimensional 20-noded solid elements C3D20 (ABAQUS, 2000) with three degree of freedoms per node, i.e., translations in axial and transverse directions *1*, *2* and *3*, respectively. The planes *1-2* and *2-3* were assumed as symmetry planes, simplifying the model mesh to 1/4 of the pipe geometry. Therefore, the weld fillet was cut in half and positioned at the symmetry plane. The length of the model was made equal to *2D* (actually *1D* considering the symmetry condition). This reduced length was enough to apply the edge loading with no implications to the stress field at the weld region.

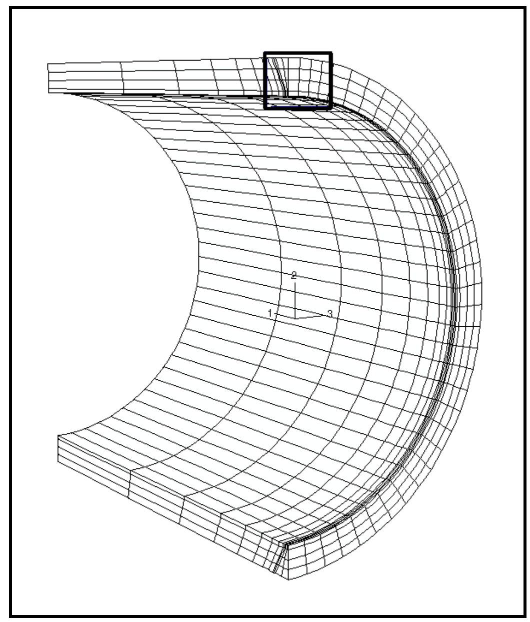

Fig. 2. The base finite element mesh with the flaw region highlighted.

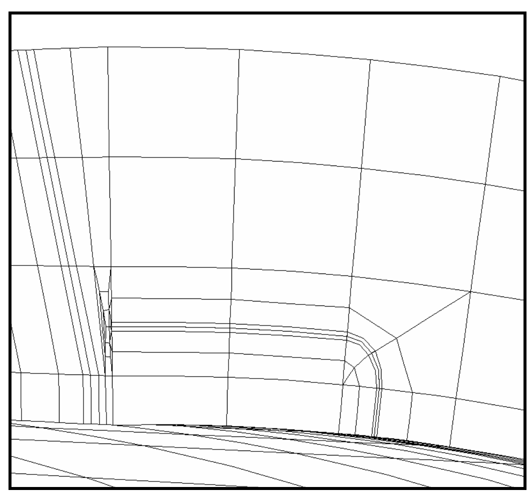

Fig. 3. Detail of the initial flaw mesh.

The finite element mesh is shown in Figs. 2~3. The former is the first base mesh on which the initial flaw was generated. In this analysis, three different base meshes were needed to propagate the flaw through the pipe thickness. The small window of Fig. 2 highlights the region of the initial flaw (Fig. 3). The elements were divided into three groups, parent material, heat affected zone and weld fillet. The mesh is more refined at the weld and HAZ, where four elements were modeled in direction *1*. The mesh of the parent material is mainly destined to transmit the edge loading to the weld region Then it was made coarse to reduce the CPU time of the analyses.

The flaw mesh was discretized using crack-blocks st19x1 and sq38x2 (ZENCRACK, 1998) that resulted in five solid elements along the crack front (11 nodes). Following the symmetry assumptions, only half crack has been modeled. Although, several refined crack-blocks are available by ZENCRACK program, the specific case of a deep crack is limited to some few options. Deep crack is defined as one in which the crack face contain crack-block elements and standard elements. The sensitivity of the mesh was not a subject of concern in this work. As soon as the experimental results are available some calibration of the mesh will be done.

Model Physical Properties

The full-scale models are API 5L X-60 grade steel pipes, which were welded using shield metal arc welding (SMAW) in the filling and gas tungsten arc welding (GTAW) at the root. The elastic properties assumed in the numerical analyses are elasticity modulus E equal to $2.1\text{x}10^5$ N/mm^2 and Poisson ratio ν equal to 0.3. The elastic-plastic properties of the material were approximated through the Ramberg-Osgood description of the uniaxial stress-strain curve (Ramberg, 1943) represented in Eq. 1. It was adopted α equal to 1.11 and 1.02, hardening parameter n equal to 16.97 and 30.51 and yield stress σ_0 equal to 486.42 N/mm^2 and 583.97 N/mm^2, for the parent material and weld fillet, respectively. The HAZ was represented with the same properties of the parent material.

$$\varepsilon = \frac{\sigma}{E}\left[1 + \alpha\left(\frac{\sigma}{\sigma_0}\right)^{n-1}\right] \tag{1}$$

The experimental crack growth data of the material was represented in the numerical model with the aid of the Paris law, i.e.

$$\frac{da}{dN} = C(\Delta K)^m , \tag{2}$$

where a is the crack growth, N is the number of fatigue cycles, C and m are material constants and ΔK is the stress intensity factor range. It was adopted C is equal to $5.37\text{x}10^{-13}$ and m is equal to 3.19. The critical intensity factor K_c was not considered in this work but it will be take into account in the future numerical-experimental correlation.

Boundary Conditions and Loading

To simulate the symmetry conditions, the normal displacements of the nodes at the plane *1-2* and plane *2-3* at $x_1=0$ were constrained to zero. The exception to these conditions is the nodes of the crack face, where the normal displacements were let free to simulate open flaw (Fig. 4). It can be observed that the constraints are defined at the nodes of the crack front but not inside the flaw.

The type of loading studied, cyclic bending moment M under constant axial loading T, was selected based on the results of the global dynamic analysis of the SCR (Pasqualino et al.,2002). This loading was applied with the aid of a reference node ($x_1=D$; $x_2=x_3=0$) that is coupled with the edge nodes of the plane *2-3* at $x_1=D$. This kinematic coupling constraint makes the set of edge nodes follow the rigid body motion of the reference node. Therefore, the bending or tension load are applied setting a moment or force at the reference node. Fig. 5 shows the deformed shape of the model under the combined loading. The thicker line represents the undeformed configuration, where the displacements were enlarged to make easy the visualization. The axial force is actuating in direction *1* and the bending moment about the axis in direction *3*.

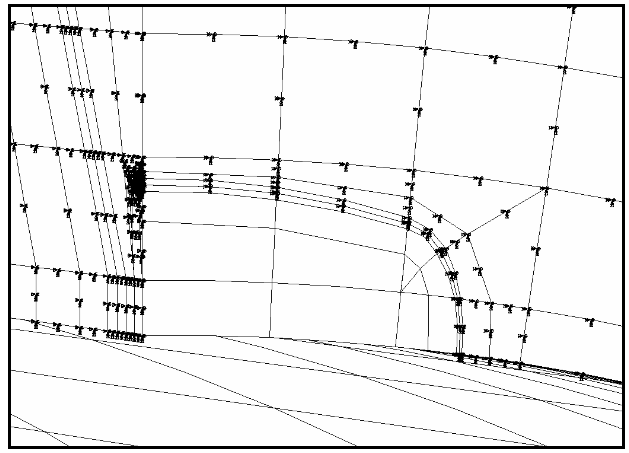

Fig.4. Boundary conditions at the flaw.

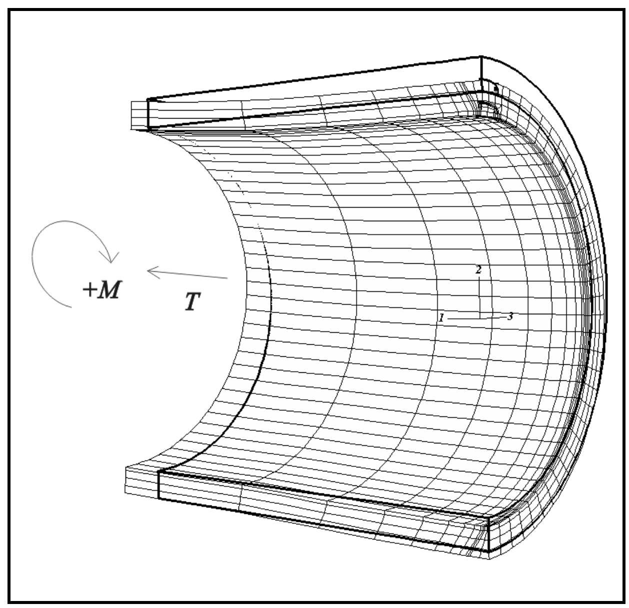

Fig. 5. Deformed configuration under combined loading of bending and tension.

The loading history (each cycle) is composed of three steps: $+M$ $+T$, $+T$ and $-M$ $+T$. The value of the bending moment is set based on the stress range S_r desired. The equation to calculate the moment as function of the normal stress σ is obtained from the theory of elastic beams,

$$M = \frac{\pi D_{sm}^2 t \sigma}{4} , \tag{3}$$

where D_{sm} is the diameter of the pipe middle surface. Then, the exact stress range is obtained at the middle surface. Three different levels of axial tension were studied: *0*, $0.05T_0$ and $0.1T_0$, where the yielding tension T_0 is given by the following equation,

$$T_0 = \pi D_{sm} t \sigma_0 \ . \tag{4}$$

The residual strains originated at the bending and straightening operation of the reeling laying process were obtained from another finite element simulation (Pasqualino and Souza, 2000). Considering a reel of 6 m of internal radius, a residual equivalent plastic strain ε^p_{eqv} equal to 0.015 was the maximum value determined at the most tensioned fibers. This accumulated strain was introduced as an initial condition on the elements of the weld.

ANALYSIS PROCEDURE

The crack growth prediction in ZENCRACK is based on the distribution of maximum energy release rate vector $\boldsymbol{G_{max}}$ along a crack front. For fatigue crack growth, the propagation law is formulated internally as a series of *da/dN* versus ΔG data. The finite element analysis provides local energy release rate values for different crack extensions at each crack front node. A numerical integration gives the direction and magnitude of crack growth at the crack front node over *N* cycles. The forward predictor integration scheme, where *dG/da* is assumed to be constant over *N* cycles, was adopted. For the case mode I (K_I), the relation between the *K* and *G* is

$$K = \left(\frac{EG}{1-\nu^2} \right)^{1/2} , \tag{5}$$

which means that the state of stress in the experimental specimen averaged over the crack front is of plane strain.

The nonlinear finite element analyses incorporate plasticity, large rotations and finite strains. Therefore, the uniaxial stress-strain curves were represented in true stress and logarithmic strains. Three finite element meshes were needed so that the flaw could cross the pipe thickness. The first, second and third base meshes carried out 5, 4 and 8 finite element analyses, respectively, to conclude this task. Figs. 6a, 6b and 6c represent the final position of the crack front at the first, second and third mesh respectively. The crack fronts obtained in the 17 analyses are show in Fig. 7, where the last one is only 0.59 mm distant from the pipe external surface.

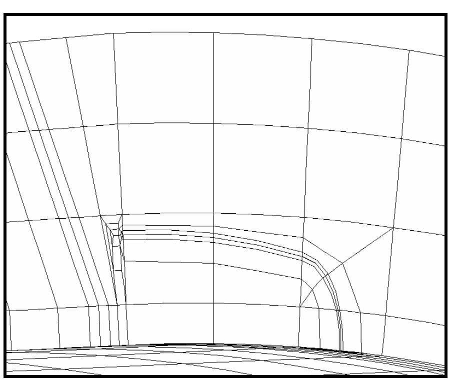

(a)

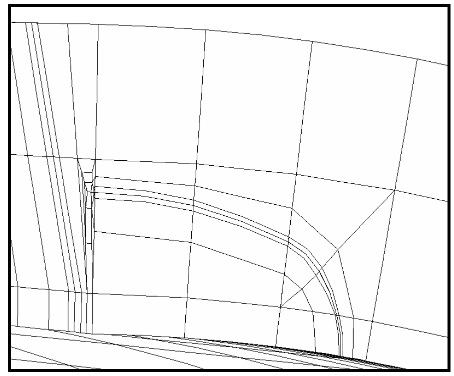

(b)

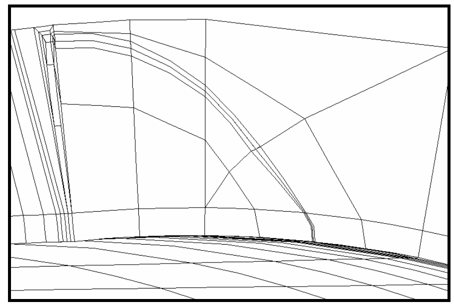

(c)

Fig.6a, b, c. The final configuration of the three different crack meshes employed in the analyses.

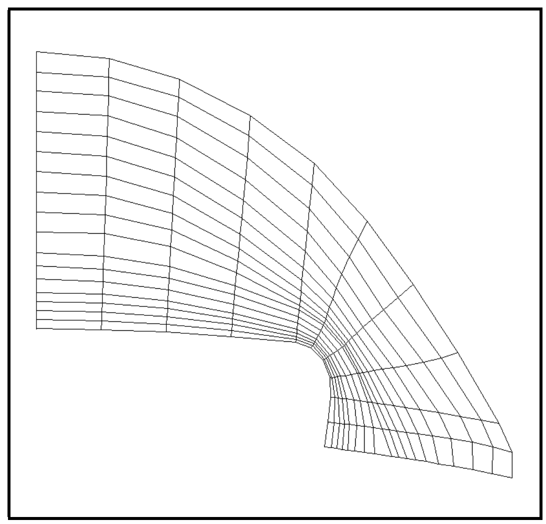

Fig. 7. The crack fronts determined during the crack propagation analysis.

RESULTS

The results are showed in Fig. 8 and Table 1. Four stress ranges S_r were needed to determine the crack growth fatigue curves, the first one with no axial tension *T* or residual strains, and three others with residual strains for tension levels equal to *0*, $0.05T_0$ and $0.1T_0$. The fatigue curves are compared with the basic S-N curve F2 (represented in Fig. 8 by the dashed line) of the British Standard code (British Standard, 1993) recommended for pipe girth welds with no backing strip. The "BSi S-N curves" furnish an estimation of the endurance of the joints under a determined stress range, including nucleation and crack propagation. Normally, the number of cycles required for crack propagation represents only one third of the fatigue life. Although they are representing different things, it is important to show that the crack propagation curves are bellow the F2 curve. The difference among these curves could be even larger if the latter did not incorporate safety factors, i.e., the F2 curve is obviously rather conservative.

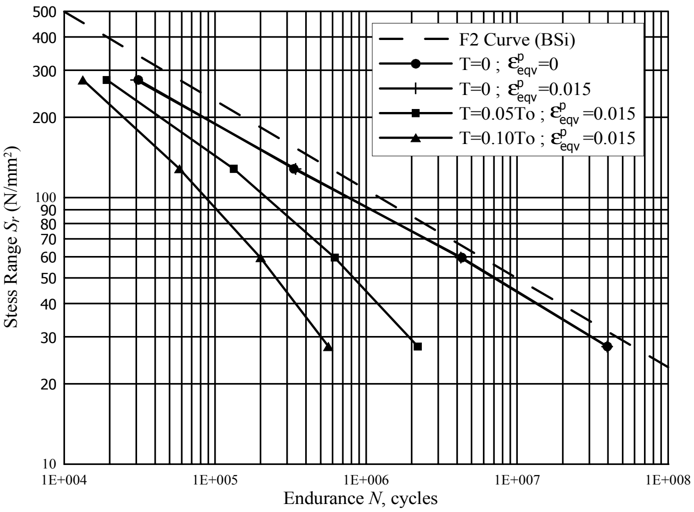

Fig. 8. Crack growth fatigue curves and F2 curve of pipe girth weld.

The points of the crack growth fatigue curves are listed in Table 1. The results of fatigue without medium stress ($T=0$) were indifferent to the presence of residual strain. The curves without tension for $\varepsilon^p_{eqv}=0$ and $\varepsilon^p_{eqv}=0.015$ are coincident in Fig 8. The slight difference between them can be verified at the first two lines of Table 1. This level of residual strain is very small if compared to the plastic strains at the crack tip (20~30%). The medium stresses showed to be a more critical parameter in this type of joint. The reduction of fatigue life is very strong even for low levels of axial tension. As verified in Fig. 8, this reduction is more critical for low stress ranges.

Table 1. Number of cycles of the crack growth analyses.

Endurance N (cycles)	S_r (N/mm^2)			
	27.6	59.5	128.1	276.0
T=.0; ε^p_{eqv}=.0	39561932	4302579	331978	30986
T=.0; ε^p_{eqv}=.015	39469492	4231569	340868	29971
T=.05T_0; ε^p_{eqv}=.015	2193345	620698	132844	19129
T=.10T_0; ε^p_{eqv}=.015	561163	200245	57961	13315

Finally, the curves of Fig. 9 show the crack growth in radial and hoop directions for the analyses with no tension or residual strain at a stress range equal to 27.6 N/mm^2. As expected, the crack grows more in radial than hoop direction because of the plane of application of the bending moment (see Fig. 5).

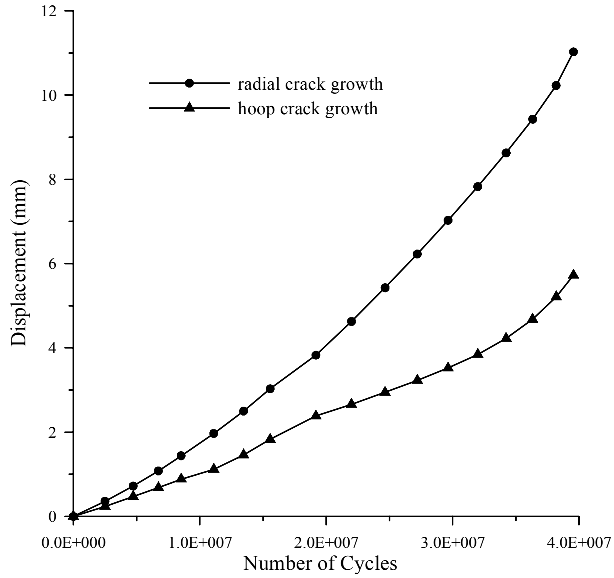

Fig. 9. Crack growth in radial and hoop directions.

CONCLUSIONS

The work comprised the development of a numerical tool to simulate the crack growth in girth welds of SCR's. Some crack growth fatigue curves considering residual strain and different levels of medium stress were obtained. The results were compared with the S-N curve F2 of BSi. As expected, the crack growth curves resulted in inferior fatigue lives than F2 curve, in spite of the conservatism of the design codes.

The results obtained were qualitatively good and showed that the fatigue life of imperfect girth welds of SCR's is strongly influenced by the axial tension (medium stress).

The residual strains generated due to the reeling laying process, for the studied case, did not affect the fatigue life of the weld. These strains are very small when compared to the plastic strains of the crack tip. However, the most dangerous effect of the reeling process has not been simulated, that is the crack growth under monotonic loading of bending and unbending. In this case, the initial flaw of the fatigue analysis would be larger, which would decrease the endurance of the joint.

The developed model must be improved through a mesh sensitivity study and a correlation of numerical and experimental results. The fatigue lives must also be checked using the experimental critical intensity factor K_c.

ACKNOWLEDGEMENTS

The numerical calculations were carried out using the framework of ABAQUS/Standard and ZENCRACK under academic license from Hibbitt, Karlsson and Sorensen, Inc. and Zentech International Ltd., respectively. The authors would like to acknowledge the financial support from PETROBRAS and FINEP from the Brazilian Ministry of Science and Technology.

REFERENCES

ABAQUS (2000). "User´s and Theory Manuals", Release 6.1, Hibbitt, Karlsson, Sorensen, Inc.

British Standard (1993). “Fatigue Design and Assessment of Steel Structures”, BS7608.

Netto, TA et al. (2000). “Fabrication of Fatigue Test and Bending Simulator Apparatus”. *Plastically Strained SCR’s Qualification Program for Installation Methods,* Part I, COPPETEC Report PENO-1292, COPPE/UFRJ, Rio de Janeiro, Brazil (restricted).

Pasqualino, IP and Souza, APF (2000). “Finite Element Model for Bending and Straightening”, *Feasibility of the Reeling Laying Process for SCR’s*, Part 1, COPPETEC Report CTPETRO-713, COPPE/UFRJ, Rio de Janeiro, Brazil (in Portuguese).

Pasqualino, IP (2001). “Models Construction”, *Feasibility of the Reeling Laying Process for SCR’s*, Part 3, COPPETEC Report CTPETRO-713, COPPE/UFRJ, Rio de Janeiro, Brazil (in Portuguese).

Pasqualino, IP, Souza, APF and Valeriano IA (2002). “Fracture Mechanics”, *Feasibility of the Reeling Laying Process for SCR’s*, Part 2, COPPETEC Report CTPETRO-713, COPPE/UFRJ, Rio de Janeiro, Brazil (in Portuguese).

Ramberg, W and Osgood, WR (1943). “Description of Stress-Strain Curves by Three Parameters”, NACA Technical Note 902.

ZENCRACK (1998). “User Manual”, Issue 6, Zentech International Ltd.